10562–10570 *Nucleic Acids Research, 2022, Vol. 50, No. 18* *Published online 26 September 2022*
https://doi.org/10.1093/nar/gkac809

Hydrazone chemistry-mediated CRISPR/Cas12a system for bacterial analysis

Anzhi Sheng[1,2], Jingyi Yang[1], Longfei Tang[1], Lili Niu[1], Liangfen Cheng[1], Yujing Zeng[3], Xu Chen[1], Juan Zhang[1,*] and Genxi Li[1,3,*]

[1]Center for Molecular Recognition and Biosensing, School of Life Sciences, Shanghai University, Shanghai 200444, PR China, [2]Department of Central Laboratory, Shanghai Chest Hospital, Shanghai Jiao Tong University School of Medicine, Shanghai 200030, PR China and [3]State Key Laboratory of Pharmaceutical Biotechnology, School of Life Sciences, Nanjing University, Nanjing 210023, PR China

Received March 23, 2022; Revised August 21, 2022; Editorial Decision September 06, 2022; Accepted September 09, 2022

ABSTRACT

In this study, a hydrazone chemistry-mediated clustered regularly interspaced palindromic repeats (CRISPR)/CRISPR-associated protein 12a (Cas12a) system has been proposed for the fist time and constructed. In our system, hydrazone chemistry is designed and employed to accelerate the formation of a whole activation strand by taking advantage of the proximity effect induced by complementary base pairing, thus activating the CRISPR/Cas12a system quickly and efficiently. Moreover, the introduction of hydrazone chemistry can improve the specificity of the CRISPR/Cas12a system, allowing it to effectively distinguish single-base mismatches. The established system has been further applied to analyze *Pseudomonas aeruginosa* by specific recognition of the probe strand with a characteristic fragment in 16S rDNA to release the hydrazine group-modified activation strand. The method shows a wide linear range from 3.8 × 10^2 colony-forming units (CFU)/ml to 3.8 × 10^6 CFU/ml, with the lowest detection limit of 24 CFU/ml. Therefore, the introduction of hydrazone chemistry may also broaden the application of the CRISPR/Cas12a system.

INTRODUCTION

Cas12a (CRISPR-associated protein 12a) is a nucleic acid endonuclease from the V-A-type clustered regularly interspaced palindromic repeats (CRISPR) system for genome editing by processing CRISPR RNAs (crRNAs) from arrays using its dedicated RNase functional domain (1,2). It can indiscriminately cleave single-stranded DNA (ssDNA) after activation of intrinsic nuclease activity by recognizing its target site, which has been used for the detection of nucleic acids (3,4). However, there are still many challenges to overcome. The system is unsuitable for distinguishing very similar ssDNA sequences (1,5). Moreover, the interference between similar ssDNA sequences may cross-react for multiple target detection in a single reaction system, which affects the analytical sensitivity and specificity (6). Usually, it may also be difficult to find a protospacer adjacent motif (PAM) sequence matching with Cas12a protein for the direct detection of short target sequences. So, the effector protein and target sequence need to be carefully selected to avoid background signals (7).

Hydrazone chemistry has the advantages of rapid reaction, mild reaction conditions and good selectivity (8,9). Since the programmability of a CRISPR/Cas system relies on the interaction of guide RNA and nucleic acid, we envisage that hydrazone chemistry can be introduced into the initiation sequence of the system to activate the CRISPR/Cas12a system more flexibly, which may not only improve the specificity, but may also be widely used in the analysis of different targets (2,10,11). Here, we have constructed a detection platform based on a hydrazone chemistry-mediated CRISPR/Cas12a system. In our system, the activation strand is subtly designed as a hairpin structure, which is elaborately split into two segments separately modified by two hydrazone-linked groups, hydrazine and an aldehyde group. Meanwhile, the probe complementary sequence is carefully designed to release the hydrazine group-modified split segment due to the specific binding of the target sequence to the probe, leading to the formation of the whole activated strand and the activation of the hydrazone chemistry-mediated CRISPR/Cas12a system. Therefore, the introduction of hydrazone chemistry not only improves the specificity of the CRISPR/Cas12a system, but also accelerates the activation process of the CRISPR/Cas12a system.

Pseudomonas aeruginosa is a common environmental bacterium that can spread rapidly through animal feces,

*To whom correspondence should be addressed. Tel: +86 25 83592510; Email: genxili@nju.edu.cn
Correspondence may also be addressed to Juan Zhang. Tel: +86 21 66137037; Email: juanzhang@shu.edu.cn

food and water. The bacterium can cause infectious diseases such as otitis, pneumonia, keratitis, sepsis and endocarditis (12). The traditional detection methods for this bacterium include colony culture and counting, which is routine, accurate and reliable for microbial detection (13,14). However, these methods are always labor-intensive and time-consuming (15), which has greatly limited their application. Therefore, it is urgent to develop a new method to detect *P. aeruginosa*. In this work, we have proposed a simple and sensitive method for the analysis of *P. aeruginosa* based on the proposed hydrazone chemistry-mediated CRISPR/Cas12a system, which may have great potential application in the future.

MATERIALS AND METHODS

Materials and reagents

All oligonucleotides (as shown in Supplementary Table S1) were synthesized and purified by Shanghai Sangon Biotechnology Co., Ltd (Shanghai, China), EnGen®LbaCas12a (Cpf1) (M0653T) was purchased from NEB (Beijing, China), RNase inhibitor (K1046) was purchased from APExBIO (Shanghai, China) and diethylpyrocarbonate (DEPC) water was purchased from Shanghai Sangon Biotechnology Co., Ltd. 4-Hydrazinobenzoic acid was obtained from Wokai Biotechnology, Co., Ltd (Beijing, China). All experimental water was obtained through the Milli-Q purification system (R >18 MΩ/cm). All other chemicals are analytical reagent grade.

Preparation of the TS1-$NHNH_2$ strand

First, 95 mg of EDC [1-ethyl-3-(3-dimethylaminopropyl)carbodiimide] and 11 mg of NHS (*N*-hydroxysuccinimide) were dissolved in 1 ml of deionized water to prepare the cross-linking agent, and then 0.5 mM 4-hydrazinobenzoic acid was added to the cross-linking agent for 20 min, followed by the addition of 100 μM TS1-NH_2 strand. After sonicating for 30 s, the mixture was kept for 12 h with regular shaking. Finally, the mixture was separated by using a gel column (illustrra MicroSpin G-25 columns) to obtain TS1-$NHNH_2$, which was characterized by Fourier infrared spectroscopy (Bertex 70, Bruker, Germany).

Hydrazone chemistry-mediated CRISPR/Cas12a system

First, the TS2-CHO strand (10 μM) was heated at 95°C for 5 min and then cooled naturally to room temperature. A 4.8 μl of the TS1-$NHNH_2$ strand (0.6 μM) was mixed with 4.8 μl of the TS2-CHO strand (0.6 μM), 8 μl of 10× buffer, 2 μl of RNase inhibitor (40 U), 3.2 μl of Cas12a (200 nM), 1.6 μl of crRNA (200 nM) and 1.6 μl of ssDNA-FAM (200 nM). Finally, DEPC water was added to a final volume of 80 μl. After incubation at 37°C for 15 min, the mixture was heated at 65°C for 10 min to inactivate the enzyme. The fluorescence intensity of the reaction solution was measured by a fluorescence spectrometer (F-7000, Hitachi Ltd, Japan).

Release of the TS1-$NHNH_2$ strand induced by synthetic target DNA

A 4.8 μl aliquot of the 16S rDNA probe strand (Probe) (0.6 μM) was mixed with 4.8 μl of the TS1-$NHNH_2$ strand (0.6 μM). After heating at 95°C for 5 min, the mixture was cooled naturally to room temperature. Subsequently, 4.8 μl of the TS2-CHO strand (0.6 μM) was added, followed by the addition of 10 μl of synthetic target DNA at various concentrations. Finally, the mixture was incubated at 37°C for 60 min. The product was characterized through polyacrylamide gel electrophoresis (PAGE).

Hydrazone chemistry-mediated CRISPR/Cas12a system for bacterial detection

Again a 4.8 μl aliquot of Probe (0.6 μM) was mixed with 4.8 μl of the TS1-$NHNH_2$ strand (0.6 μM), and the mixture was heated at 95°C for 5 min and cooled naturally to room temperature. Subsequently, 4.8 μl of the TS2-CHO strand (0.6 μM) and 10 μl of *P. aeruginosa* suspension at various concentrations were added and incubated at 37°C for 60 min, followed by the addition of 8 μl of 10× buffer, 2 μl of RNase inhibitor (40 U), 3.2 μl of Cas12a (200 nM), 1.6 μl of crRNA (200 nM) and 1.6 μl of ssDNA-FAM (200 nM). Finally, DEPC water was added to give a final volume of 80 μl. After incubating at 37°C for 15 min, the mixture was heated at 65°C for 10 min to inactivate the enzyme. The fluorescence intensity of the reaction solution was measured by a fluorescence spectrometer (F-7000, Hitachi Ltd, Japan). The logarithm of odds (LOD) of the assay was calculated using the formula $LOD = 3\sigma/S$, where σ is the standard deviation of the unadded sample and S is the slope of the calibration curve.

Performance evaluation of the established method

All strains were obtained from stock cultures in the laboratory of Professor Dr Lili Niu. The concentrations of these strains were determined by McFarland's turbidimetric assay. The specificity of the established method was evaluated using 3.8×10^6 colony-forming units (CFU)/ml of *Escherichiacoli* 2571, *E. coli* 25922 and *Stapylococcus aureus* instead of *P. aeruginosa*. In addition, different concentrations of *P. aeruginosa* (3.8×10^3, 3.8×10^5 and 3.8×10^6 CFU/ml) were added to pure water, milk, grapefruit juice and green tea to make the spiked samples. After adjusting the pH value of the spiked samples with NaOH or HCl to 7.0, the amount of *P. aeruginosa* was analyzed by using the established method, and the relative recoveries were calculated.

Fluorescence *in situ* hybridization through 16S rDNA Probe

A single colony of bacteria was cultured in LB medium for 9 h and examined under a microscope. Subsequently, 50 μl of the solution was taken evenly onto the slide, and successively fixed by flame and 4% paraformaldehyde (PFA) for 10 min, followed by drying naturally. Then the glass slide was immersed in a mixture of 50% alcohol and 50% phosphate-buffered saline (PBS) for 10 min and air-dried. After that,

200 μl of Probe-Cy5 was added and incubated at 55°C for 6 h in hybridization buffer containing 10 mmol/l NaCl, 30% (v/v) formamide, 5 mmol/l Na_2EDTA, 0.2% (v/v) Triton X-100 and 50 mmol/l Tris–HCl. After hybridization, the slide was washed twice for 10 min each time with 55°C pre-warmed washing buffer containing 5 mmol/l Tris–HCl, 15 mmol/l NaCl and 0.1% (v/v) Triton X-100. The slices were air-dried naturally and sealed with 80 μl of antifade polyvinylpyrrolidone mounting medium, followed by covering with a coverslip.

Statistical analysis

Two-tailed Student's *t*-test was used for evaluating statistical differences between two groups by the GraphPad software (Prism 7), and $P < 0.05$ was statistically significant.

RESULTS AND DISCUSSION

Hydrazone chemistry-mediated CRISPR/Cas12a system

The hydrazone chemistry-mediated CRISPR/Cas12a system is illustrated in Figure 1A. The activated strand is split into two parts, i.e. TS1-$NHNH_2$ and TS2-CHO. Neither TS1-$NHNH_2$ nor TS2-CHO can activate the CRISPR/Cas12a system. With the aid of complementary base pairing, TS1-$NHNH_2$ containing a hydrazide group is easier to react with the aldehyde group of TS2-CHO to form a whole TS1/TS2 strand through a hydrazone bond. Localization of Cas protein mainly depends on the PAM in TS1-$NHNH_2$ (2). After the linkage of the TS1-$NHNH_2$ strand with the TS2-CHO strand, the Cas12a/crRNA complex localizes to the TS1/TS2 strand and cleaves to generate sticky ends far away from its PAM sequence (16). The subsequent activated trans-cleavage activity of the Cas12a/crRNA complex will result in the non-specific cleavage of ssDNA-FAM and fluorescence recovery.

The formation of TS1/TS2 through a hydrazone bond was confirmed by infrared spectroscopy. The peaks at 1563 cm^{-1} and 1266 cm^{-1} corresponding to the amide II and III bands and another peak at 1642 cm^{-1} attributed to the stretching vibration of the C=N double bond appear, while the peaks at 1735 cm^{-1} ascribed to the stretching of the carbonyl group in the saturated aliphatic aldehyde disappears (Supplementary Figure S1A). These results confirm the formation of a hydrazone bond between TS1-$NHNH_2$ and TS2-CHO. Moreover, a new band in L3 can be observed (Supplementary Figure S1B), verifying the successful linkage between TS1-$NHNH_2$ and TS2-CHO.

Slight changes in the target sequence can lead to instability of the triple complex of the target DNA–crRNA–Cas effector interfering with the activation response (16,17). We first explored the effect of strand length on CRISPR/Cas12a activation. When the number of bases of TS1 or TS2 changes from 8 nt to 11 nt, no obvious fluorescence peaks can be detected (Figure 1B1, B2), indicating that none of them could activate CRISPR/Cas12a. When the number of bases of TS1 or TS2 increases from 12 nt to 20 nt (18), obvious fluorescence peaks can be detected, indicating the occurrence of partially activated CRISPR/Cas12a (Figure 1B1, B2). Based on these findings, in the following experiment, the full-length TS was split into two segments, namely TS1-$NHNH_2$ and TS2-CHO, each with a length of 10 nt.

Subsequently, the effects of the introduction of hydrazone chemistry on the activation of CRISPR/Cas12a were investigated. Compared with that for the full-length TS, the whole TS1/TS2 can give similar values of K_{cat}, K_m and the k_{cat}/K_m ratio (Figure 1C1, C2). These results suggest that the introduction of hydrazone chemistry does not affect the activated effect of the whole TS1/TS2 on the CRISPR/Cas12a system and its corresponding trans-cleavage activity.

It has been reported that double-stranded activated CRISPR/Cas12a is insensitive to single-base mismatches (19). Along with the optimization of the Cas12a concentration (Supplementary Figure S2), we further investigated the effect of introduction of hydrazone chemistry on the specificity of the CRISPR/Cas12a system. In comparison with that of full-length TS with one mismatched base pair (Figure 1D1), obviously decreased mean fluorescence intensity can be found for the whole TS1/TS2 with one pair of mismatched bases (Figure 1D2). This can be explained by the fact that the mismatched bases influence the occurrence of complementary base pairing between TS1-$NHNH_2$ and TS2-CHO, so as to reduce the proximity effect and hinder the formation of a hydrazone bond. As confirmed by our previous experiment, TS1-$NHNH_2$ or TS2-CHO with a length of 10 nt cannot activate the CRISPR/Cas12a system (Figure 1B1, B2). Therefore, the whole TS1/TS2 with one pair of mismatched bases evidently can influence the extent of the activation of the CRISPR/Cas12a system and its corresponding trans-cleavage efficiency. The introduction of hydrazone chemistry can improve the specificity of the CRISPR/Cas12a system, which can effectively distinguish a single-base mismatch in the target sequence.

The degree of mismatch tolerance is highly dependent on the source of the effector protein and the location of the mismatch (18). We have further investigated the influence of the mismatch position on the trans-cleavage activity of the CRISPR/Cas12a system. For a single-base mismatch, different positions (1, 5, 10, 15 and 20 relative to the PAM region) were selected to study their effect on the trans-cleavage activity, and the corresponding results are shown in Supplementary Figure S3. With mismatch at position 1 adjacent to the PAM region, an obvious statistical differences can be found for both full-length TS and whole TS1/TS2. This can be explained by the fact that the PAM region is extremely important for the recognition and activation of the CRISPR/Cas12a system. However, for a single-base mismatch located at other positions, an evident statistical difference can only be observed for the whole TS1/TS2, while for the full-length TS no difference is found when the mismatch position is >5 away from the PAM region (3,20). These can be attributed to the weakened proximity effect as a result of a single-base mismatch, which is a disadvantage for the formation of a hydrazone bond and the ensuing whole TS1/TS2. Therefore, the introduction of hydrazone chemistry reduces the tolerance and increases the sensitivity of the CRISPR/Cas12a system activated by a single-base mismatched TS. Moreover, a decrease in cross-reactivity can be found for the hydrazone-linked whole TS1/TS2 in comparison with that for the full-length TS. As shown in

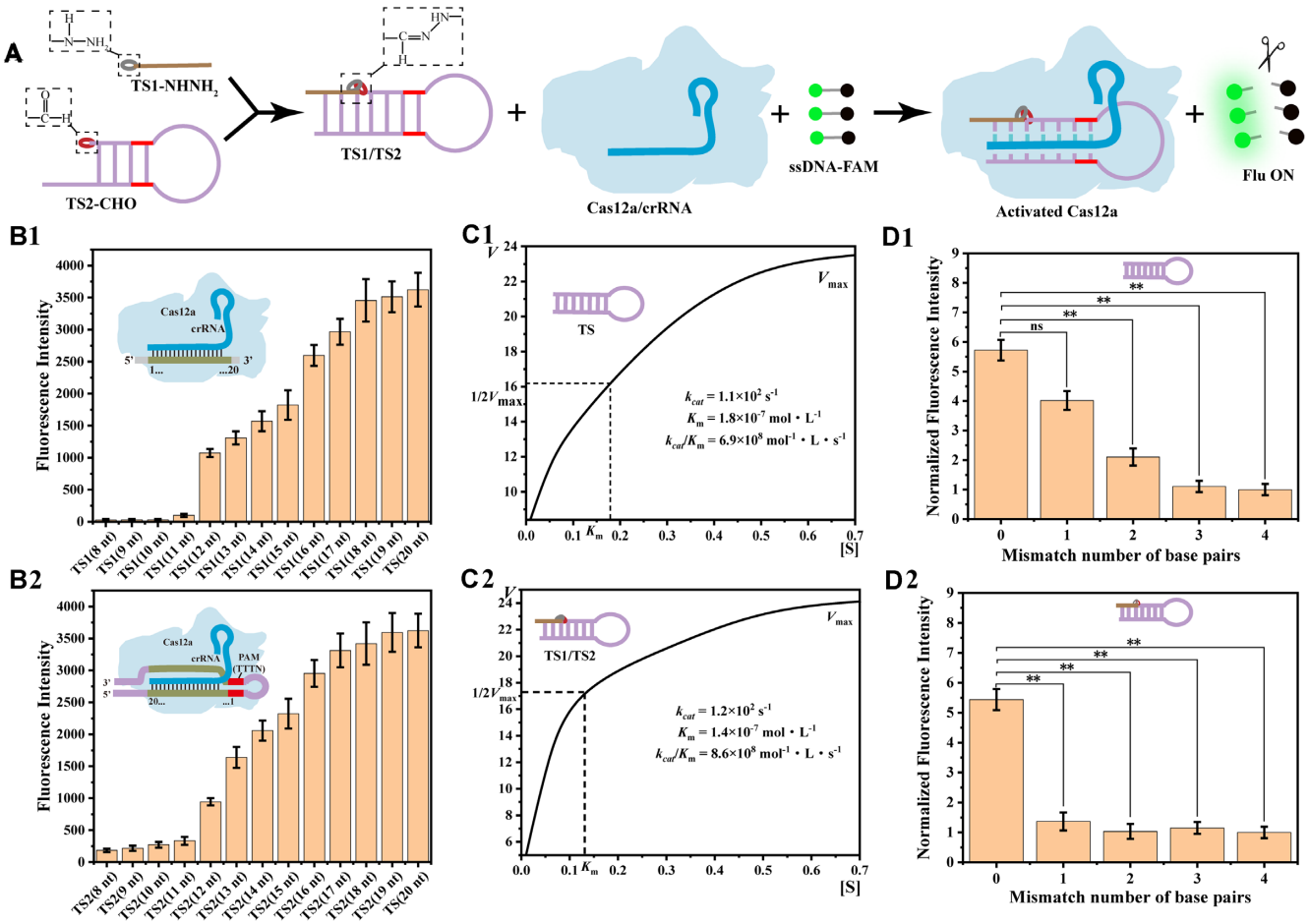

Figure 1. Hydrazone chemistry-mediated CRISPR/Cas12a system. (**A**) Schematic illustration of the CRISPR/Cas12a system mediated by hydrazone chemistry. Fluorescence spectra with different base numbers of (**B1**) TS1 or (**B2**) TS2. Reaction rate versus the concentration of substrate strand for (**C1**) the full-length TS- or (**C2**) the whole TS1/TS2-activated Cas12a. Histograms of trans-cleavage of Cas12a activated by (**D1**) the full-length TS or (**D2**) the whole TS1/TS2 with a different number of mismatched base pairs. Statistical significance was calculated by two-tailed Student's *t*-test. ns, non-significant; $^{**}P < 0.01$. Error bars represent the standard deviations of three independent experiments ($n = 3$).

Supplementary Figure S4, the single-base mismatched mutants make the full-length TS produce a high fluorescence background. In contrast, almost no effect can be found for hydrazone-linked whole TS1/TS2. These results signify that the introduction of a hydrazone bond can increase the specificity of the CRISPR/Cas12a system.

Synthetic target DNA mediated the formation of the TS1/TS2 strand

Figure 2A shows that synthetic target DNA induces the formation of the TS1/TS2 strand. Target DNA can competitively bind with Probe, resulting in the occurrence of a strand displacement reaction and the release of TS1-$NHNH_2$. The released TS1-$NHNH_2$ strand will bind to TS2-CHO through complementary base pairing. By virtue of the proximity effect, the hydrazine group of TS1-$NHNH_2$ and the aldehyde group of TS2-CHO will react to form a hydrazone bond. In turn, the formed hydrazone bond accelerates the occurrence of complementary base pairing. Finally, hybrid strand TS1/TS2 will form through the hydrazone bond. In contrast, the strand displacement reaction will not occur and TS1/TS2 will not form without synthetic target DNA. As shown in Figure 2B, a new band in L4 indicates the formation of a Probe/TS1-$NHNH_2$ hybrid. Moreover, the new band at the top of L5 can be explained by the formation of TS1/TS2 through a hydrazone bond. In the absence of Target, two bands in L6 can be separately ascribed for Probe/TS1-$NHNH_2$ and TS2-CHO, suggesting no occurrence of a strand displacement reaction. In the presence of Target, two new bands shown in red squares belong to TS1/TS2 and Probe/Target, respectively.

We further utilize the trans-cleavage capability of CRISPR/Cas12a to confirm the formation of TS1/TS2. As shown in Figure 2C, almost no fluorescence peak can be found with separate addition of Probe/TS1-$NHNH_2$, TS2-CHO or Target, as a result of no formation of TS1/TS2 to activate the CRISPR/Cas12a system. In contrast, compared with that for full-length TS, a similar fluorescence peak can be found with the addition of Target into the mixture of Probe/TS1-$NHNH_2$ and TS2-CHO. The result confirms the formation of TS1/TS2 resulting from the strand displacement reaction. Moreover, the band of long-stranded DNA (LDNA) as the substrate

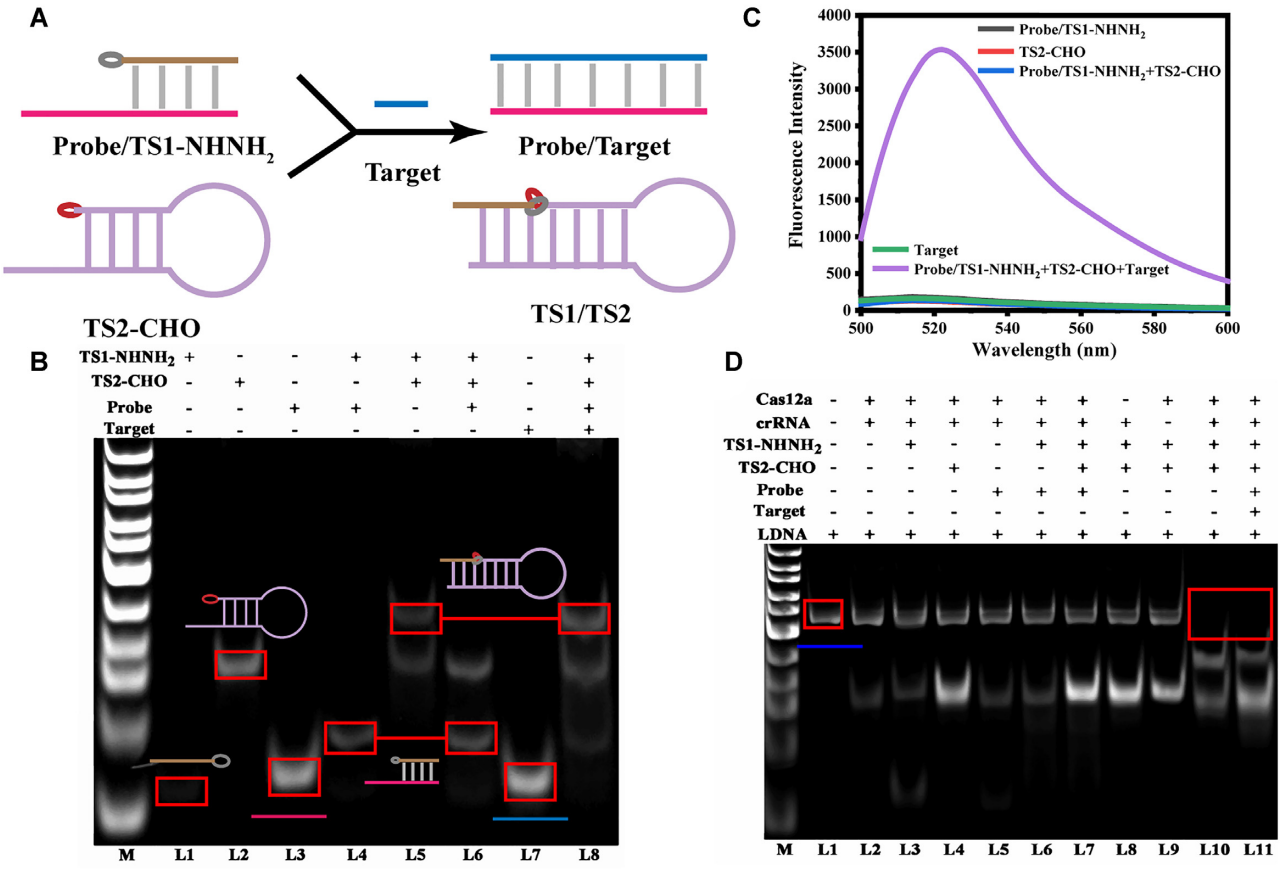

Figure 2. Synthetic target DNA mediated the formation of the TS1/TS2 strand. (**A**) Schematic illustration of the release of TS1-$NHNH_2$ induced by target binding and the formation of TS1/TS2 through hydrazone chemistry. (**B**) PAGE image for the strand displacement reaction. M, DNA marker; L1, TS1-$NHNH_2$; L2, TS2-CHO; L3, Probe; L4, Probe/TS1-$NHNH_2$; L5, TS1-$NHNH_2$/TS2-CHO; L6, Probe/TS1-$NHNH_2$ + TS2-CHO; L7, Target; L8, Probe/TS1-$NHNH_2$ + TS2-CHO + Target. (**C**) Fluorescence spectra for trans-cleavage of CRISPR/Cas12a in the presence of different strands. (**D**) PAGE image for trans-cleavage of CRISPR/Cas12a. M, DNA marker; L1, long-stranded DNA (LDNA); L2, Cas12a/crRNA + LDNA; L3, Cas12a/crRNA + TS1-$NHNH_2$ + LDNA; L4, Cas12a/crRNA + TS2-CHO + LDNA; L5, Cas12a/crRNA + Probe + LDNA; L6, Cas12a/crRNA + Probe/TS1-$NHNH_2$ + LDNA; L7, Cas12a/crRNA + Probe/TS1-$NHNH_2$ + TS2-CHO + LDNA; L8, crRNA + TS1-$NHNH_2$ + TS2-CHO + LDNA; L9, Cas12a + TS1-$NHNH_2$ + TS2-CHO + LDNA; L10, Cas12a/crRNA + TS1/TS2 + LDNA; L11, Cas12a/crRNA + Probe/TS1-$NHNH_2$ + TS2-CHO + Target + LDNA.

of CRISPR/Cas12a trans-cleavage disappears with the addition of Target in L11 in comparison with that without the addition of Target in L7 (Figure 2D). In addition, the LDNA band also vanishes in the presence of TS1/TS2. These results are in good agreement with those obtained through fluorescence spectroscopy and verify that the synthetic target DNA can mediate the formation of the TS1/TS2 strand.

Mechanism of bacterial analysis based on the hydrazone chemistry-mediated CRISPR/Cas12a system

The principle of the hydrazone chemistry-mediated CRISPR/Cas12a system for bacterial analysis is illustrated in Figure 3. With highly conserved regions across species and species-specific variable regions, bacterial 16S rRNA gene (16S rDNA) sequences are usually utilized for the identification of various bacteria (21). As shown in Figure 3, 16S rDNA can competitively bind with the Probe from the Probe/TS1-$NHNH_2$ hybrid, resulting in the release of TS1-$NHNH_2$ and the formation of Probe/16S rDNA. The released TS1-$NHNH_2$ can hybridize with TS2-CHO through complementary base pairing, so as to accelerate the formation of TS1/TS2 through a hydrazone bond between the hydrazine group of TS1-$NHNH_2$ and the aldehyde group of TS2-CHO. The formed TS1/TS2 can activate Cas12a/crRNA to discriminately cleave ssDNA-FAM, resulting in the recovery of fluorescence. In contrast, in the absence of bacteria, the formation of TS1/TS2 will not happen and the fluorescence will not recover.

After smearing and Gram staining, the slender Gram-negative bacilli with variable lengths as well as bluntly rounded ends in the form of spherical rods or threads can be observed under light microscopy (Image a, Figure 3B), which could be characterized as *P. aeruginosa*. Meanwhile, the red fluorescence can be found for *P. aeruginosa* by using the 16S rDNA gene probe (22) labeled with the Cy5 fluorescent moiety (Image b, Figure 3B). The result signifies that the probe can be successfully applied for bacterial

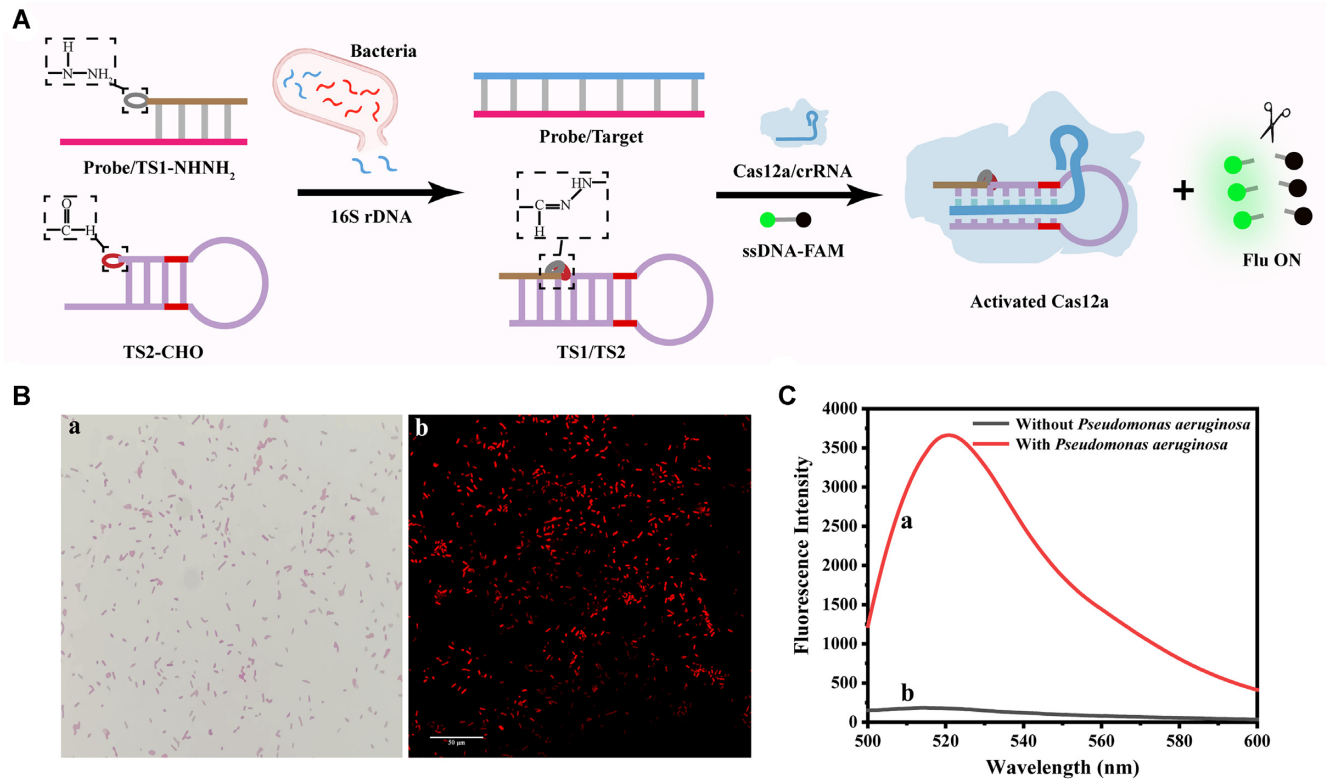

Figure 3. Mechanism of bacterial analysis based on the hydrazone chemistry-mediated CRISPR/Cas12a system. (**A**) Schematic illustration for bacterial analysis based on the hydrazone chemistry-mediated CRISPR/Cas12a system. (**B**) (a) Microscopic image of *P. aeruginosa* and (b) fluorescence imaging analysis of *P. aeruginosa* by using the 16S rDNA gene probe strand. (**C**) Fluorescence spectra obtained (a) with and (b) without *P. aeruginosa*.

analysis. Furthermore, almost no fluorescence peak can be observed without *P. aeruginosa* (Image b, Figure 3C). In contrast, an evident high fluorescence peak can be found in the presence of *P. aeruginosa* (Image a, Figure 3C). The results clearly demonstrate that *P. aeruginosa* can induce the formation of TS1/TS2 to activate CRISPR/Cas12a, leading to the recovery of fluorescence. Meanwhile, the control experiment was designed and conducted, and the corresponding results are shown in Supplementary Figure S5. Almost no change of fluorescence intensity can be observed for TS1 or TS2, implying that TS1 or TS2 cannot activate the CRISPR/Cas12a system. High fluorescence intensity can be found for TS1 + TS2 and TS1-$NHNH_2$ + TS2-CHO, confirming the activation of the CRISPR/Cas12a system. However, a higher activation efficiency can be found for TS1-$NHNH_2$ + TS2-CHO in comparison with that of TS1 + TS2, considering that the former gives a quicker reaction rate (745.94 mol/l/s), a higher maximized fluorescence intensity (4126.80) and a shorter time needed to reach steady state (10 min) than those (130.70 mol/l/s, 3792 and 14 min) of the latter. The results verify that the formation of a hydrazone bond between the hydrazine group of TS1-$NHNH_2$ and the aldehyde group of TS2-CHO can accelerate the formation of the whole TS1/TS2, so as to efficiently activate the CRISPR/Cas12a system. Therefore, the established method based on the hydrazone chemistry-mediated CRISPR/Cas12a system can be developed to detect bacteria.

Quantitative analysis of bacteria based on the hydrazone chemistry-mediated CRISPR/Cas12a system

As shown in Figure 4A, we first quantitatively analyzed the synthesized DNA Target strand using the established method. As the concentration of the synthetic DNA Target strand increases from 0 nM to 100 nM, the fluorescence intensity at 520 nm gradually increases (Figure 4A). The presence of the Target allows the release of TS1-$NHNH_2$ from the Probe/TS1-$NHNH_2$ double hybrid, culminating in the formation of the hydrazone bond-mediated hybridized TS1/TS2, which activates the trans-cleavage activity of CRISPR/Cas12a. It has been further found that the fluorescence intensity values increase linearly with increased logarithmic values of the synthetic DNA Target strand concentrations from 0.1 nM to 100 nM (Figure 4B). A linear equation: $I = 1021.37 + 903.85 \times \log C_{\text{Target}}$ can be fitted, and the lowest detection limit has been calculated to be 0.074 nM ($3\sigma/S$), which is lower than other reported values for the detection of synthetic DNA (23,24). By calculating the slope of the three regression equations for the concentrations of the synthetic DNA Target strand from 0 nM to 100 nM, a relative standard deviation (RSD) value of 3.7% could be obtained, and the results indicate the good precision of our established method.

Subsequently, on the basis of quantitative analysis of synthetic DNA Target, we used the established method to quantitatively analyze the bacteria which have been deter-

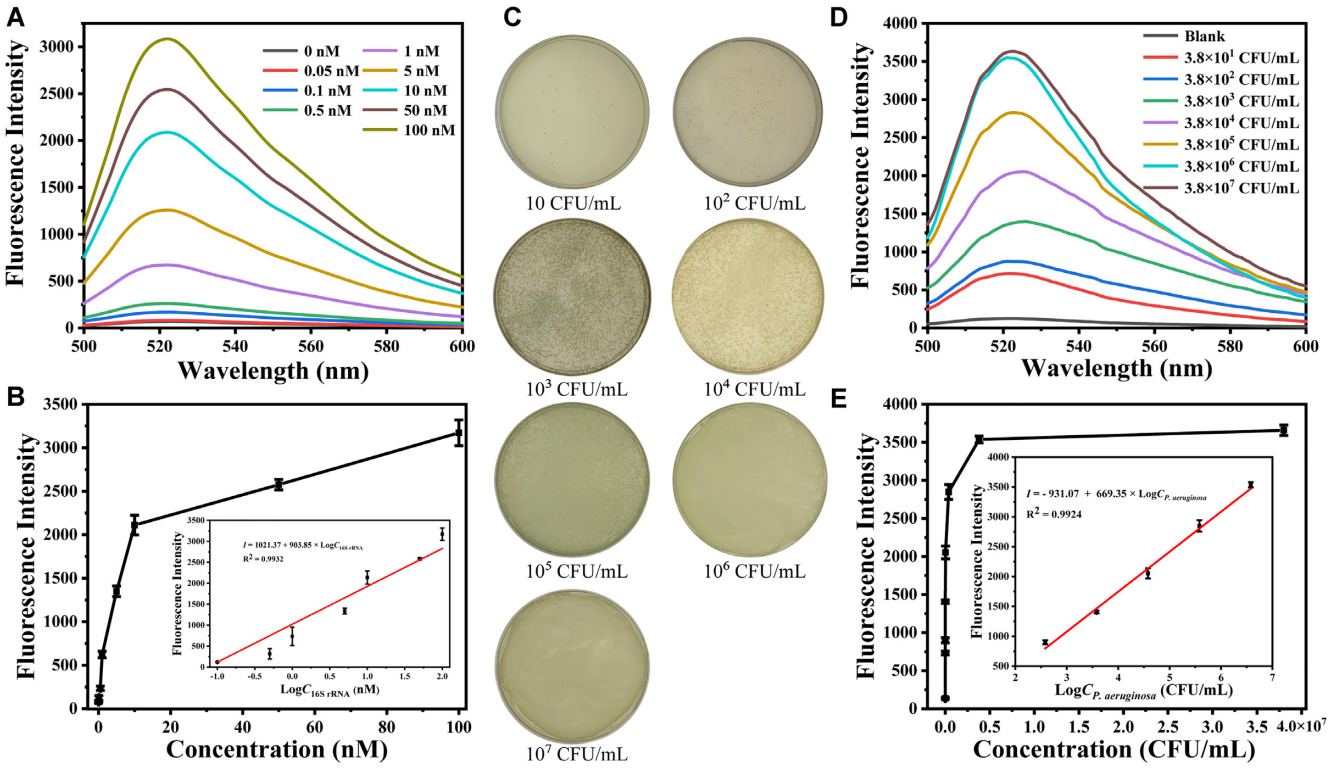

Figure 4. Quantitative analysis of bacteria based on the hydrazone chemistry-mediated CRISPR/Cas12a system. (**A**) Fluorescence spectra with different concentrations of synthetic DNA Target strands. (**B**) The relationship between fluorescence intensity and the concentration of the synthesized DNA Target strand. Inset: the linear relationship between the fluorescence intensity and the logarithm value of the concentration of the synthetic DNA Target strand. (**C**) Counting of *P. aeruginosa* by the dilution coating plate method. (**D**) Fluorescence spectra with different concentrations of bacteria. (**E**) The relationship between the fluorescence intensity and the concentration of bacteria. Inset: the linear relationship between the fluorescence intensity and logarithmic value of the concentration of bacteria. Error bars represent the standard deviations of three independent experiments ($n = 3$).

mined by the dilution coating plate method (Figure 4C). As the amounts of bacteria increase from 3.8×10^1 to 3.8×10^7 CFU/ml, the fluorescence intensities gradually increase (Figure 4D). The fluorescence intensity increases linearly as the logarithmic values of bacterial concentration increased from 3.8×10^2 to 3.8×10^6 CFU/ml. The linear equation $I = -931.07 + 669.35 \times \log C_{P.\ aeruginosa}$ ($R^2 = 0.9924$) can be obtained (Figure 4E), with a linear detection range wider than the reported value (Supplementary Table S2) (25,26). The calculated detection limit is 24 CFU/ml ($3\sigma/S$), which is lower than the previously reported value (26–28). In addition, an RSD value of 6.6% can be obtained, which indicates the good reproducibility of the established method.

Performance evaluation of the established method based on the hydrazone chemically assisted CRISPR/Cas12a system

Different bacteria have been used to validate the specificity of the established method for the analysis of *P. aeruginosa*. Gram staining has been used to identify different bacteria. As shown in Figure 5A, different bacteria have different morphological characteristics. Moreover, red fluorescence can only be observed for *P. aeruginosa* (Figure 5B), and the result confirms the specific capturing of the designed 16S rDNA gene Probe on *P. aeruginosa*. Meanwhile, a low fluorescence intensity can be observed for *E. coli* 2571, *E. coli* 25922 and *S. aureus* (Figure 5C). In contrast, *P. aeruginosa* exhibits high fluorescence intensity. These results demonstrate the high specificity of the established method for the detection of *P. aeruginosa*. This can be attributed to the high selectivity of the 16S rDNA gene Probe for the detection of *P. aeruginosa*. To verify the practicability of the method, we use pure water, milk, grapefruit juice and green tea from a local supermarket as the sample sources to spike with different concentrations of *P. aeruginosa*. As shown in Figure 5D and Supplementary Table S3, the relative recovery varies between 90% and 110%, with a relative error of <8.7%, indicating that the constructed method can be used to analyze *P. aeruginosa* in real samples.

The hydrazone chemistry-mediated CRISPR/Cas12a system can be easily used for the detection of other target genes, due to the sequence programmability of the target binding domain in the DNA probe. The hydrazone chemistry-mediated CRISPR/Cas12a system has been explored for the detection of *S. aureus*, and the corresponding experimental results are shown in Supplementary Figures S6, S7 and S8. Supplementary Figure S6 illustrates the detection principle of *S. aureus* through the hydrazone chemistry-mediated CRISPR/Cas12a system. Probe2 can specifically bind with TS3-$NHNH_2$ to form Probe2/TS3-$NHNH_2$ through complementary base pairing. 16S rDNA from *S. aureus* can bind with Probe2 through a strand displacement reaction, resulting in the release of TS3-

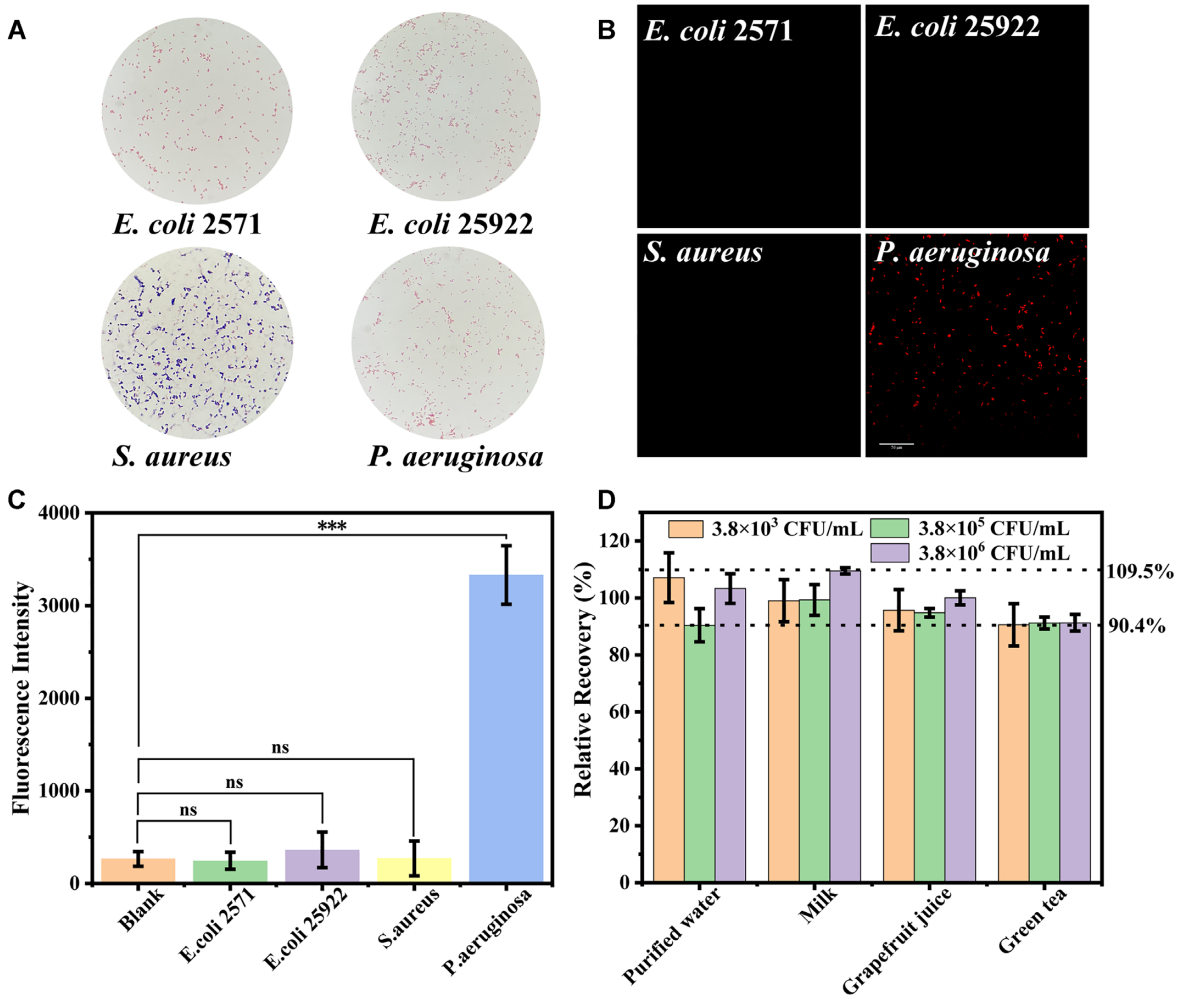

Figure 5. Performance evaluation of the established method. (**A**) Gram staining of different bacteria. (**B**) Fluorescence *in situ* imaging of different bacteria by using a fluorescent 16S rDNA gene probe. (**C**) Fluorescence intensity in the presence of different bacteria. (**D**) Recovery analysis of the established method. Error bars represent the standard deviations of three independent experiments ($n = 3$). (ns, non-significant; ***$P < 0.001$.)

$NHNH_2$. With the formation of the hydrazine linkage, the released TS3-$NHNH_2$ can react with TS4-CHO to give TS3/TS4, which can activate the CRISPR/Cas12a system so as to produce the fluorescence signal. The designed Probe2 can be successfully applied to image *S. aureus* (Supplementary Figure S7). Moreover, as shown in Supplementary Figure S8, in the absence of *S. aureus*, no fluorescent signal can be observed, confirming the stability of TS3-$NHNH_2$ and TS4-CHO. In contrast, a high fluorescence peak appears in the presence of *S. aureus*. Therefore, the hydrazone chemistry-mediated CRISPR/Cas12a system can be developed to analyze *S. aureus*. These results signify that the system could be universal and can be used for other target genes. Additionally, almost no fluorescence can be found when using a scrambled sequence (s-Probe3) instead of the designed sequence (Probe2), confirming good specificity of the established method. Thus it can be seen that the hydrazone chemistry-mediated CRISPR/Cas12a system not only has good stability and universality, but also has good specificity for indirect detection of non-nucleic acid targets.

CONCLUSIONS

In conclusion, we have constructed a hydrazone chemistry-mediated CRISPR/Cas12a system and have explored its ability to distinguish single-base mismatches. Taking advantage of the proximity effect generated by complementary base pairing, the formation of hydrazone bonds can be accelerated. In view of its modularity and unique structural property, the pervasive and versatile hydrazone chemistry can link the split activated strand to the whole activated strand, so as to activate the CRISPR/Cas12a system effectively. Based on the system, a highly sensitive detection platform has been further developed and applied for bacterial detection. The developed platform is simple and sensitive, with a low detection limit and good specificity. Moreover, the platform can not only be applied for the detection of 16S rDNA in bacteria, but can also serve for direct detection of nucleic acid targets with the help of an aptamer or probe-based recognition cascade reaction. Meanwhile, the platform can also provide a stable and cost-effective assay system for indirect detection of other non-nucleic acid targets. So, the introduction of hydrazone chemistry can also

broaden the scope of application of the CRISPR/Cas12a system.

DATA AVAILABILITY

All data supporting the findings of this study are available within the article and its supplementary information, or will be made available from the authors upon request.

SUPPLEMENTARY DATA

Supplementary Data are available at NAR Online.

ACKNOWLEDGEMENTS

The authors greatly thank the Genxi Li/Juan Zhang lab group for discussion of the project.

FUNDING

This work is sponsored by the Science and Technology Commission of Shanghai Municipality [20392001800] and the National Natural Science Foundation of China [31671923].
Conflict of interest statement. None declared.

REFERENCES

1. Li,S.Y., Cheng,Q.X., Liu,J.K., Nie,X.Q., Zhao,G.P. and Wang,J. (2018) CRISPR-Cas12a has both *cis*- and *trans*-cleavage activities on single-stranded DNA. *Cell Res.*, **28**, 491–493.
2. Anzalone,A.V., Koblan,L.W. and Liu,D.R. (2020) Genome editing with CRISPR-Cas nucleases, base editors, transposases and prime editors. *Nat. Biotechnol.*, **38**, 824–844.
3. Dai,Y., Somoza,R.A., Wang,L., Welter,J.F., Li,Y., Caplan,A.I. and Liu,C.C. (2019) Exploring the trans-cleavage activity of CRISPR-Cas12a (cpf1) for the development of a universal electrochemical biosensor. *Angew. Chem. Int. Ed.*, **58**, 17399–17405.
4. Cheng,L., Yang,F., Tang,L., Qian,L., Chen,X., Guan,F., Zhang,J. and Li,G. (2022) Electrochemical evaluation of tumor development via cellular interface supported CRISPR/Cas trans-cleavage. *Research (Wash DC)*, **2022**, 9826484.
5. Kim,D., Kim,J., Hur,J.K., Been,K.W., Yoon,S.H. and Kim,J.S. (2016) Genome-wide analysis reveals specificities of cpf1 endonucleases in human cells. *Nat. Biotechnol.*, **34**, 863–868.
6. van Dongen,J.E., Berendsen,J.T.W., Steenbergen,R.D.M., Wolthuis,R.M.F., Eijkel,J.C.T. and Segerink,L.I. (2020) Point-of-care CRISPR/Cas nucleic acid detection: recent advances, challenges and opportunities. *Biosens. Bioelectron.*, **166**, 112445.
7. Li,S.Q., Li,X., Xue,W., Zhang,L., Yang,L.Z., Cao,S.M., Lei,Y.N., Liu,C.X., Guo,S.K., Shan,L. *et al.* (2021) Screening for functional circular RNAs using the CRISPR-Cas13 system. *Nat. Methods*, **18**, 51–59.
8. Hang,H.C. and Bertozzi,C.R. (2001) Chemoselective approaches to glycoprotein assembly. *Acc. Chem. Res.*, **34**, 727–736.
9. Chen,T., Sheng,A., Hu,Y., Mao,D., Ning,L. and Zhang,J. (2019) Modularization of three-dimensional gold nanoparticles/ferrocene/liposome cluster for electrochemical biosensor. *Biosens. Bioelectron.*, **124-125**, 115–121.
10. Broughton,J.P., Deng,X.D., Yu,G.X., Fasching,C.L., Servellita,V., Singh,J., Miao,X., Streithorst,J.A., Granados,A., Sotomayor-Gonzalez,A. *et al.* (2020) CRISPR-Cas12-based detection of SARS-CoV-2. *Nat. Biotechnol.*, **38**, 870–874.
11. Yu,Y., Li,W., Gu,X., Yang,X., Han,Y., Ma,Y., Wang,Z. and Zhang,J. (2022) Inhibition of CRISPR-Cas12a trans-cleavage by lead (II)-induced G-quadruplex and its analytical application. *Food Chem.*, **378**, 131802.
12. Silby,M.W., Winstanley,C., Godfrey,S.A.C., Levy,S.B. and Jackson,R.W. (2011) *Pseudomonas* genomes: diverse and adaptable. *FEMS Microbiol. Rev.*, **35**, 652–680.
13. Yu,Q., Zhai,L.G., Bie,X.M., Lu,Z.X., Zhang,C., Tao,T.T., Li,J.J., Lv,F.X. and Zhao,H.Z. (2016) Survey of five food-borne pathogens in commercial cold food dishes and their detection by multiplex PCR. *Food Control*, **59**, 862–869.
14. Jain,S., Chattopadhyay,S., Jackeray,R., Abid,C.K.V.Z., Kohli,G.S. and Singh,H. (2012) Highly sensitive detection of *Salmonella typhi* using surface aminated polycarbonate membrane enhanced-ELISA. *Biosensors. Bioelectron.*, **31**, 37–43.
15. Zhang,X.Y., Wu,T.T., Yang,Y.M., Wen,Y.Q., Wang,S.T. and Xu,L.P. (2020) Superwettable electrochemical biosensor based on a dual-DNA walker strategy for sensitive *E. coli* O157:H7 DNA detection. *Sens. Actuators B Chem.*, **321**, 112271.
16. Dai,Y., Wu,Y., Liu,G. and Gooding,J.J. (2020) CRISPR mediated biosensing toward understanding cellular biology and point-of-care diagnosis. *Angew. Chem. Int. Ed.*, **59**, 20754–20766.
17. Sheng,A.Z., Wang,P., Yang,J.Y., Tang,L.F., Chen,F. and Zhang,J. (2021) MXene coupled with CRISPR-Cas12a for analysis of endotoxin and bacteria. *Anal. Chem.*, **93**, 4676–4681.
18. van Dongen,J.E., Berendsen,J.T.W., Eijkel,J.C.T. and Segerink,L.I. (2021) A CRISPR/Cas12a-assisted in vitro diagnostic tool for identification and quantification of single CpG methylation sites. *Biosens. Bioelectron.*, **194**, 113624.
19. Chen,J.S., Ma,E., Harrington,L.B., Da Costa,M., Tian,X., Palefsky,J.M. and Doudna,J.A. (2018) CRISPR-Cas12a target binding unleashes indiscriminate single-stranded DNase activity. *Science*, **360**, 436–439.
20. Zhang,W., Shi,R., Dong,K., Hu,H., Shu,W., Mu,Y., Yan,B., Li,L., Xiao,X. and Wang,H. (2022) The off-target effect of CRISPR-Cas12a system toward insertions and deletions between target DNA and crRNA sequences. *Anal. Chem.*, **94**, 8596–8604.
21. Chung,H.J., Castro,C.M., Im,H., Lee,H. and Weissleder,R. (2013) A magneto-DNA nanoparticle system for rapid detection and phenotyping of bacteria. *Nat. Nanotechnol.*, **8**, 369–375.
22. Wellinghausen,N., Kothe,J., Wirths,B., Sigge,A. and Poppert,S. (2005) Superiority of molecular techniques for identification of Gram-negative, oxidase-positive rods, including morphologically nontypical *Pseudomonas aeruginosa*, from patients with cystic fibrosis. *J. Clin. Microbiol.*, **43**, 4070–4075.
23. Mao,X., Jiang,J.H., Xu,X.M., Chu,X., Luo,Y., Shen,G.L. and Yu,R.Q. (2008) Enzymatic amplification detection of DNA based on 'molecular beacon' biosensors. *Biosens. Bioelectron.*, **23**, 1555–1561.
24. Loaiza,O.A., Campuzano,S., Pedrero,M. and Pingarron,J.M. (2007) DNA sensor based on an *Escherichia coli lac Z* gene probe immobilization at self-assembled monolayers-modified gold electrodes. *Talanta*, **73**, 838–844.
25. Zhao,J.W., Zhu,W.J. and He,F.J. (2005) Rapidly determining *E. coli* and *P. aeruginosa* by an eight channels bulk acoustic wave impedance physical biosensor. *Sens. Actuators B Chem.*, **107**, 271–276.
26. Jia,F., Xu,L., Yan,W.J., Wu,W., Yu,Q.Q., Tian,X.J., Dai,R.T. and Li,X.M. (2017) A magnetic relaxation switch aptasensor for the rapid detection of *Pseudomonas aeruginosa* using superparamagnetic nanoparticles. *Mikrochim. Acta*, **184**, 1539–1545.
27. Yamaguchi,N., Kitaguchi,A. and Nasu,M. (2012) Selective enumeration of viable enterobacteriaceae and *Pseudomonas* spp. in milk within 7 h by multicolor fluorescence in situ hybridization following microcolony formation. *J. Biosci. Bioeng.*, **113**, 746–750.
28. Yue,H., He,Y., Fan,E., Wang,L., Lu,S.G. and Fu,Z.F. (2017) Label-free electrochemiluminescent biosensor for rapid and sensitive detection of *Pseudomonas aeruginosa* using phage as highly specific recognition agent. *Biosens. Bioelectron.*, **94**, 429–432.